ELSEVIER

NeuroImage

www.elsevier.com/locate/ynimg
NeuroImage 25 (2005) 734–745

Neuromagnetic localization of rhythmic activity in the human brain: a comparison of three methods

M. Liljeström,* J. Kujala, O. Jensen,[1] and R. Salmelin

Brain Research Unit, Low Temperature Laboratory, Helsinki University of Technology, P.O. Box 2200, Fin-02015 HUT, Espoo, Finland

Received 22 April 2004; revised 4 October 2004; accepted 29 November 2004
Available online 24 February 2005

Cortical rhythmic activity is increasingly employed for characterizing human brain function. Using MEG, it is possible to localize the generators of these rhythms. Traditionally, the source locations have been estimated using sequential dipole modeling. Recently, two new methods for localizing rhythmic activity have been developed, Dynamic Imaging of Coherent Sources (DICS) and Frequency-Domain Minimum Current Estimation (MCE_{FD}). With new analysis methods emerging, the researcher faces the problem of choosing an appropriate strategy. The aim of this study was to compare the performance and reliability of these three methods. The evaluation was performed using measured data from four healthy subjects, as well as with simulations of rhythmic activity. We found that the methods gave comparable results, and that all three approaches localized the principal sources of oscillatory activity very well. Dipole modeling is a very powerful tool once appropriate subsets of sensors have been selected. MCE_{FD} provides simultaneous localization of sources and was found to give a good overview of the data. With DICS, it was possible to separate close-by sources that were not retrieved by the other two methods.

Keywords: MEG; Oscillations; Spatial filter; DICS; MCE; Dipole modeling; Source localization

Introduction

Neuronal populations in the resting human brain generate macroscopic oscillatory activity, typically in the frequency range from 8 to 25 Hz, which can be detected outside the head with neurophysiological imaging techniques [electroencephalography (EEG) and magnetoencephalography (MEG)]. The *alpha rhythm*, peaking at about 10 Hz, is recorded over the posterior parts of the brain (Adrian and Matthews, 1934; Berger, 1929). Source areas in the parietooccipital sulcus and in the calcarine fissure are indicated by electrocorticographic (Perez-Borja et al., 1962) and MEG studies (Salenius et al., 1995; Salmelin and Hari, 1994a). The *mu rhythm*, with both 10-Hz and 20-Hz components, is found in the primary somatosensory and motor cortices (Chatrian et al., 1959; Gastaut, 1952; Salmelin et al., 1995; Tiihonen et al., 1989). In some individuals, *tau rhythm* from the auditory cortex can be detected as well, with frequencies somewhat below 10 Hz (Lehtelä et al., 1997; Niedermeyer, 1990; Tiihonen et al., 1991). Despite the often-used term *spontaneous* activity, cortical rhythms exhibit task-dependent and stimulus-dependent reactivity. For example, the alpha rhythm is strongest when the subject has his eyes closed and is dampened when the subject opens his eyes. Even visual imagery suffices to temporarily suppress the alpha activity (Salenius et al., 1995). The mu rhythm, on the other hand, is dampened by limb movements and tactile stimulation. Suppression of the mu rhythm during movement is often followed by a brief burst of 20 Hz activity above resting level (Salmelin and Hari, 1994b). Rhythmic activity also changes with the behavioral state (attentive, drowsy, sleeping), and various diseases induce changes in frequency, amplitude, or reactivity of cortical rhythms (Niedermeyer, 1993).

Localization of ongoing oscillatory activity is important for establishing the normal spatial and spectral variation of cortical rhythmicity in the healthy human brain, and for characterizing abnormal changes induced, e.g., by stroke (Mäkelä et al., 1998). For estimation of the overall level of rhythmic activity, particularly when comparisons are made between areas or experimental conditions, localization of the generators of rhythmic activity is essential. For example, if the subject is tilting his head so that the left hemisphere is closer to the sensors than the right hemisphere is, one might erroneously deduce that cortical rhythms are stronger in the left than right hand area when, at the cortical level, the strengths are equal. When investigating task-related modulation of rhythmic activity, a rough estimate of the timing of suppression/rebound can be obtained by inspecting the sensors that show the largest modulation. However, for accurate description of timing, one needs to localize the (possibly multiple) areas which generate the rhythmic activity. Once the separate sources have been

* Corresponding author. Fax: +358 9 4512969.
E-mail address: mia.liljestrom@hut.fi (M. Liljeström).
[1] Present address: F.C. Donders Centre for Cognitive Neuroimaging, 6525 EK Nijmegen, The Netherlands.
Available online on ScienceDirect (www.sciencedirect.com).

1053-8119/$ - see front matter © 2005 Elsevier Inc. All rights reserved.
doi:10.1016/j.neuroimage.2004.11.034

localized, the time course of activity can be determined in each of these areas and the task-related modulation may thus be computed at the cortical level. Localization of rhythmic activity from MEG data has helped to demonstrate, e.g., that the 10-Hz and 20-Hz components in the sensorimotor cortex are, at least partly, separate phenomena. Generators of the 20-Hz rhythm tend to be located anteriorly, extending into the motor cortex, whereas the 10-Hz rhythm concentrates to the sensory side in the parietal cortex (Salmelin and Hari, 1994b). Furthermore, movement-related modulation of the 10-Hz activity occurs around the hand representation area for finger, mouth, and toe movements, whereas the 20-Hz modulation follows the representation of each body part along the motor cortex (Salmelin et al., 1995).

Until recently, cortical sources of rhythmic activity have typically been identified using a standard approach where one assumes that the underlying source currents can be represented by a single equivalent current dipole (ECD). Using this approach, the non-averaged MEG data is band-pass filtered and single ECDs are computed every 10–20 ms with a least-squares fit to a chosen subset of sensors (Salmelin and Hari, 1994a). Covering the entire cortex requires 5–7 different subsets of sensors. The ECDs cluster in areas producing oscillatory activity. Since no averaging has been applied, the locations of the dipoles are highly affected by noise. Hence, the source cluster represents a statistical distribution of the most likely source area. Several source areas can be distinguished when they do not overlap in time and/or space and when the directions of current flow differ sufficiently (Hämäläinen et al., 1993). A great advantage of finding the sources of oscillatory activity in the time domain is that any variation of source areas at different times is readily detected. A clear disadvantage, on the other hand, is that the subsets of sensors must be chosen with some care to include the interesting areas but not to be too extensive, to facilitate efficient modeling with single ECDs. The entire brain cannot be searched at once. The selection of subsets of sensors is fairly straightforward, e.g., when one is interested in the sensorimotor rhythms. In these cases, the ECD approach has, indeed, been very successful. For instance, sources of motor cortical 20-Hz activity synchronized with electromyogram from a moving body part have been localized with this approach (Salenius et al., 1997). It is also possible to distinguish the 20-Hz modulation in the hand and face motor representations (Salmelin and Sams, 2002) during mouth movements. Using the ECD approach, the relative contributions from the hand and face areas during speech production were shown to differ between fluent speakers and stutterers (Salmelin et al., 2000). However, selection of the relevant subsets of sensors becomes quite difficult when the spatial and spectral distribution differs from the normal pattern, and requires that a highly experienced researcher generates the models by trial and error.

During the past few years, new types of approaches have been proposed which identify source areas of rhythmic activity in the frequency domain, simultaneously from the whole brain, without explicit assumptions about the number of sources. Jensen and Vanni (2002) have developed a method utilizing minimum-current estimates in the frequency domain (MCE_{FD}). The data are divided into subsections in time, and a Fourier transformation is applied. The minimum-current estimates (MCEs; Matsuura and Okabe, 1995; Uutela et al., 1999) are calculated separately for the real and the imaginary parts and averaged. An estimate of the source currents is obtained, which explains most of the data while minimizing the absolute sum of the currents with respect to the L_1-norm. As an L_1 minimum-norm approach is employed, a solution with a few distinct source points is favored. MCE does not assume any specific structure for the sources, such as dipolarity.

Gross et al. (2001), on the other hand, have designed a spatial filter in the frequency domain. Spatial filters are designed to pass activity from a certain spatial location, while attenuating activity or noise originating from other locations, using a weighted sum of the sensor signals (Van Veen et al., 1997). Dynamic Imaging of Coherent Sources (DICS) was primarily designed for investigating coherence between neuronal populations but can be used also for localizing sources of rhythmic activity. Localization of correlated sources is typically considered a problem in beamformer techniques (Van Veen et al., 1997). With highly coherent sources, the minimum distance required to separate two sources using DICS increases, but the sources can still be separated if the signal-to-noise ratio is high (Gross et al., 2001). In practice, oscillatory sources between distant areas are not expected to reach a level of coherence that would cause problems in the analysis. DICS is a linearly constrained minimum variance beamformer which allows computation of power and coherence at any given location in the brain. For localizing the sources of rhythmic activity, a three-dimensional grid that covers the entire brain is defined, and the power is calculated at each grid point. The resulting image, thresholded and color coded according to noise-normalized power, is referred to as a power statistical parametric map (pSPM). No assumptions are made about the number of active sources. A similar approach, synthetic aperture magnetometry (SAM), utilizing a nonlinear minimum-variance beamformer (Robinson and Vrba, 1999), has been used to compare the amount of rhythmic activity between different experimental conditions (see, e.g., Cheyne et al., 2003; Singh et al., 2002; Taniguchi et al., 2000).

With these new methods emerging, characterization of rhythmic activity promises to become more of a routine procedure in MEG data analysis, thus opening up interesting new ways to investigate human brain function. Analysis of rhythmic activity allows for new experimental designs in MEG with ongoing, natural tasks. However, choosing the appropriate tool for analyzing the data can be difficult. It is therefore necessary to compare the methods and discuss the underlying assumptions. Here, we evaluate and compare the performance and reliability of the traditional ECD approach, MCE_{FD}, and DICS on spatio-spectral analysis of real data from four healthy subjects, and on simulations constructed on the basis of the real data sets.

Materials and methods

MEG recordings

MEG data were collected from four subjects in four experimental conditions: when they were relaxed, with eyes closed (ec) and eyes open (eo), and when they lifted the left index finger (lf) or the right index finger (rf). During these types of tasks, oscillatory activity is usually detected around the hand sensorimotor cortex, the parietooccipital sulcus, and the calcarine sulcus. These rhythms are particularly strong when the subject is fully relaxed, with his eyes closed. This condition would thus seem ideal for localizing the cortical sources of rhythmic activity. However, the parietooccipital rhythm is often so strong that localization of the more frontal, and generally weaker, sensor-

imotor rhythms becomes difficult. The posterior 'visual' rhythms can be largely suppressed by opening the eyes. Both the eyes-closed and eyes-open conditions were therefore used for localizing generators of spontaneous rhythms. Motor tasks can be employed to transiently increase the sensorimotor rhythmic activity, and thus potentially improve source localization. Finger movements are often used both for localizing the hand areas from evoked responses and also for evaluating the reactivity of the hand sensorimotor rhythms.

Spontaneous activity was recorded for 3 min during the eyes-closed and eyes-open conditions. The finger movements were paced by a 1-kHz tone presented to the left ear, with an interstimulus interval (ISI) of 3–5 s. Each movement was repeated approximately 60–80 times, thus resulting in a total recording time of approximately 5 min. The subjects had their eyes open during the measurements of finger movements.

The cerebral magnetic fields were recorded in a magnetically shielded room using a Vectorview whole-head magnetometer (Neuromag Ltd., Helsinki, Finland). The Vectorview system has 306 channels arranged along the surface of a helmet in an array of 102 different locations, each with 2 planar gradiometers and 1 magnetometer. Only the gradiometers were taken into account in the data analysis.

The recording passband was 0.03–200 Hz and the signals were digitized at 600 Hz. The data was down-sampled to 300 Hz and stored for off-line analysis. For each condition a 150 s stretch was used for the data analysis. Spherically symmetric conductor models were obtained from the individual MR images.

Simulations

The simulated data was designed to resemble real data as well as possible. The source areas were represented by current dipoles. An Equivalent Current Dipole (ECD) is a good approximation for a small active region. Although the sources in real data are not true current dipoles but have a certain spatial extent the field patterns measured a few centimeters from the actual source region are essentially dipolar (Hämäläinen et al., 1993). In practical situations, the ECD has proven to be a very efficient model for describing the cortical sources of both responses evoked by stimuli or tasks and rhythmic activity (e.g., Hari and Salmelin, 1997; Lounasmaa et al., 1996). The time series for the simulated sources were obtained by filtering white noise using a first-order filter, and the signal was then modulated to 10 Hz. By this approach a time-dependent signal with frequencies centered on 10 Hz was obtained, with both amplitude and phase changing as a function of time. Different time series were used for each simulated source so that the amplitude and phase at a given time instant differed between two active sources. Fig. 1 shows the time series and power spectra of the simulated data. The forward problem (computation of the magnetic field starting from the source currents) was solved using a realistically shaped single compartment boundary element model (BEM) (Hämäläinen and Sarvas, 1989).

The noise was obtained from a recording without a subject ('empty room'-measurement) and added to the signal obtained from the forward modeling. Different signal-to-noise ratios were obtained by changing the amplitude of the source, with standard deviations ranging from 2 nAm to 15 nAm. The simulated data sets were constructed after the measured data had been analyzed, placing sources near areas where activity had been identified in the real data.

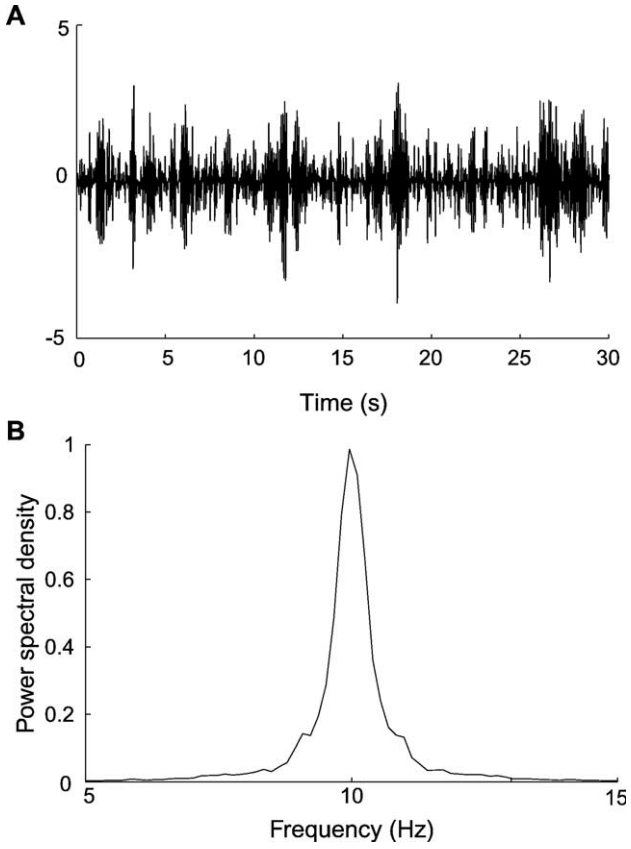

Fig. 1. Simulated data. (A) Time series and (B) power spectra of the simulated source.

Data analysis

Frequency spectra

The frequency ranges that contain the dominant rhythmic activity were identified from the amplitude spectra for the sensors. The frequency passbands were determined individually for each subject. Typically, one frequency range around 10 Hz and one around 20 Hz were chosen. In dipole modeling and DICS, the same frequency intervals with bandwidths of 3–5 Hz were used. In the MCE_{FD} software, the bandwidth can be selected only by varying the size of the fast Fourier Transform (FFT). A frequency resolution of approximately 0.6 Hz was considered reasonable, and several frequencies close to the highest spectral peaks within the intervals used in dipole modeling and DICS were chosen. Fig. 2 shows the averaged amplitude spectra for all subjects for a sensor over the left and over the right sensorimotor area as well as for a sensor over the posterior parietal region. Two frequency bands were used for Subjects 1, 2, and 4, corresponding to the main peaks in the spectra. For Subject 3, three frequency bands were used.

Dipole modeling

The data were band-pass filtered around the frequency bands of interest identified from the frequency spectra. The sources were modeled as Equivalent Current Dipoles. Only one dipole was assumed to be active at a given time point. The location, strength, and orientation of the ECD were determined at consecutive 10-ms intervals, corresponding to approximately 10 dipoles per cycle for the 10-Hz activity and 5 dipoles per cycle for the 20-Hz activity.

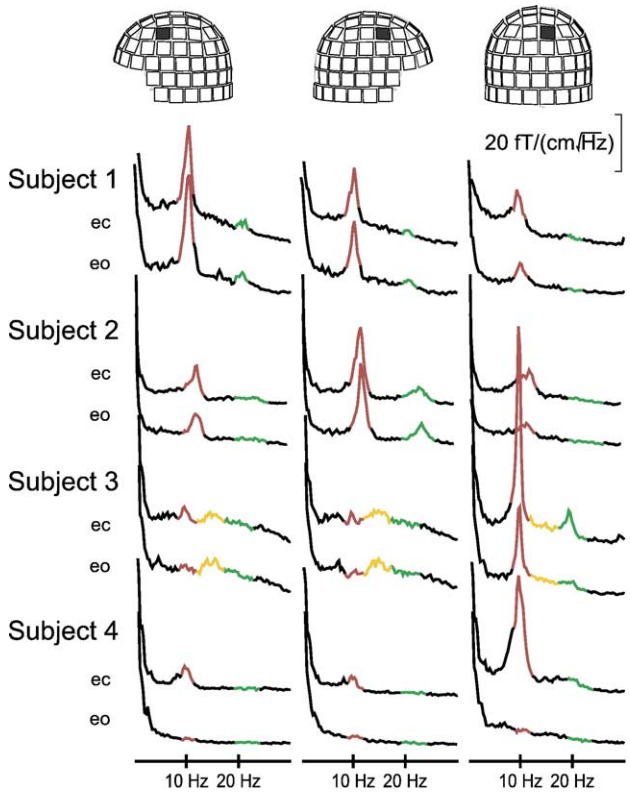

Fig. 2. Frequency spectra for all subjects in the eyes-closed (ec) and eyes-open (eo) conditions. Sensors over the left hand area, over the right hand area and over posterior parietal regions are shown. The selected frequency bands are color coded.

A spherically symmetric conductor model was used in the calculations.

Five different sensor subsets for localizing ECDs were chosen for each subject: sensors over the left rolandic area, the right rolandic area, the parietooccipital area, the vertex, and the frontal areas. The conditions used in this study have been well described in the literature and the choice of subsets was thus based on experience from earlier studies (e.g., Salmelin and Hämäläinen, 1995; Salmelin and Hari, 1994a) as well as on the amplitude spectra. The exact extent of the subsets of sensors was selected separately for each subject due to interindividual variance in spatial distribution of spectral peaks, as well as different head position with respect to the sensors. Approximately 40–60 sensors were used in each subset.

The goodness of fit (g value; Kaukoranta et al., 1986) and the confidence volume were calculated for each dipole. Only ECDs with a g value exceeding 80% and with a 95% confidence volume below 100 mm^3 were accepted, provided that they were located beneath the area covered by the selected subset of detectors. The dipole clusters are shown as color-coded dipole density plots superimposed on the individual MR images. The dipole density plots show the areas with the highest concentration of dipoles, but disregard any information on the direction of current flow.

DICS

The data were segmented into sections of 256 samples and a Hanning window was applied to reduce spectral leakage. FFT was applied to the data segments, giving a frequency resolution of approximately 1.2 Hz. With a larger FFT size, the correlation matrix becomes too large and cannot be computed using the existing software. The cross-spectral density was computed between all combinations of MEG signals and averaged over the whole time span. The diagonal elements in the cross-spectral matrix consist of the power of the sensors. The mean power for the selected frequency bands, centered at 10 Hz and 20 Hz, was extracted and the spatial filter was applied for each grid point (Gross et al., 2001). The power at a certain grid point was computed from the solution to the forward problem at the respective grid point and the extracted signal power. Two orthogonal dipolar sources were used in the calculations of the forward problem. The search volume was restricted to the brain, thereby ensuring that the localized sources were inside the brain, and speeding up the process considerably. The shape of the brain was obtained from the MR images of each subject. Uniform noise power was assumed in all sensors, and the noise was projected through the spatial filter by replacing the cross-spectral matrix by the noise cross-spectral matrix. Since the noise is used as a scaling factor, the magnitude of the noise is irrelevant; only the spatial distribution is important. The power was then noise normalized, interpolated to the millimeter MRI resolution and displayed superimposed on the MR images as a power statistical parametric map (pSPM). A spherically symmetric conductor model was used for the forward calculations.

Initially, the strongest source areas were identified using a grid with a 12-mm side length, covering the entire brain. A more accurate estimate for the source location was found by using a 4-mm grid restricted to an area with a 2-cm radius around an identified source. As a source has been localized, it can subsequently be removed by including the field produced by this source in the noise estimate before noise normalization. Here, only the principal direction of the current flow was taken into account. One could also remove all activity in that location (all directions of current flow), but in that case, two close-by sources may be difficult to separate. After the removal, the second strongest source becomes the most conspicuous one and can be readily detected. This approach was used to identify the strongest oscillatory sources.

MCE_{FD}

The data were down-sampled to 150 Hz in order to save disk space. Frequencies were selected from the maxima in the amplitude spectra. A few different frequencies around 10 Hz and 20 Hz were chosen in order to ensure that no source areas were missed. For each sensor, the data were divided into subsections with 50% overlap. A Hanning window was applied to reduce spectral leakage before applying the Fourier transformation. An FFT size of 256 was considered appropriate (Jensen and Vanni, 2002), corresponding to a frequency resolution of approximately 0.6 Hz. The minimum-current estimates (Uutela et al., 1999) were calculated separately for the real and the imaginary data, and averaged. A realistic boundary-element model (BEM) of a standard brain was used to restrict the search volume to the brain. The possible source locations were constrained to a grid with a 10-mm side length. Locations closer than 30 mm to the center of the conductor model were excluded. A spherical conductor model was used for calculating the gain matrix. In order to reduce the variance, the current estimate is regularized using singular value decomposition. The cutoff index of the regularization, i.e., the number of accepted singular values, was 30. The results were first shown projected to the surface of the BEM for an overview of the

data. From this overview, the regions of interest were selected and viewed as ellipsoids superimposed on the individual MR images. In this study, both of these formats are used depending on which one is more informative.

Results

Measured data

Two main groups of sources were found: sources near parietooccipital areas and sources near primary sensorimotor areas. Comparisons between the three methods were easier for sources near the hand areas as they typically originate from a very restricted area. Near the parietooccipital sulcus and in the occipital lobe, several sources that are located quite close to each other can be active simultaneously, thus making source localization somewhat ambiguous. Some additional sources were also found, especially using DICS.

Activation in the hand area

The results were very similar for the three methods. The differences in location between the methods were only a few millimeters in data with good signal-to-noise ratio, and up to 2 cm in data with very poor signal-to-noise ratio. The same sources were found using all tasks (eyes open, eyes closed, finger right, and finger left). Subjects 1 and 2 showed typical mu rhythm and all three methods found sources in the hand area in both the 10-Hz and 20-Hz frequency bands (see Table 1). Fig. 3 shows the sources localized in the sensorimotor areas for Subject 1 in the 10-Hz and the 20-Hz frequency bands during the eyes-closed condition. In Subject 3, sources were found in the hand area mainly in the 15-Hz and 20-Hz frequency bands (see Table 1). Subject 4 showed very little rhythmic activity (see frequency spectra in Fig. 2), and sources could not be found using any of the three methods.

Parietooccipital sources

The differences between the three methods were larger in the posterior regions than in the sensorimotor areas and the number of localized sources and exact locations varied. Typically, sources were found around the parietooccipital sulcus, near the midline, and in the occipital areas (Figs. 4A and B). In the eyes-closed condition, separate sources could be identified in the left and right occipital regions with DICS. With MCE_{FD} and dipole modeling, the strongest activity was found near the parietooccipital sulcus, close to the midline. With dipole modeling, sources in parietal and occipital areas could in some cases be separated according to the orientation of current flow (Fig. 4A). During the eyes-open condition, the posterior 10-Hz activity was suppressed and could not be separated from noise using MCE_{FD} in two of the subjects

Table 1
Sources in the hand area

		DICS	MCE_{FD}	Dipoles	DICS	MCE_{FD}	Dipoles
Subject 1			10 Hz			20 Hz	
RH	eo	(40,17,90)	(41,14,84)	(39,13,84)	(38,13,86)	(42,9,88)	–
	ec	(40,14,85)	(39,15,88)	(39,16,85)	(36,14,83)	(41,9,90)	(35,15,84)
	lf	(36,17,85)	(38,12,87)	(39,16,87)	(33,18,89)	(29,11,92)	–
	rf	(39,13,86)	(38,12,86)	(39,14,86)	(36,14,85)	(36,9,91)	(39,4,91)
LH	eo	(−40,4,86)	(−41,9,90)	(−41,8,87)	(−34,10,86)	(−37,13,94)	(−38,11,88)
	ec	(−41,7,85)	(−42,9,88)	(−42,9,87)	(−33,14,85)	(−36,13,93)	(−41,8,88)
	lf	(−44,4,86)	(−42,9,88)	(−44,9,88)	(−37,9,86)	(−38,11,87)	(−42,9,88)
	rf	(−41,7,86)	(−40,10,86)	(−42,8,86)	(−36,9,86)	(−37,14,93)	(−38,16,89)
Subject 2			10 Hz			20 Hz	
RH	eo	(36,10,93)	(36,14,93)	(39,14,97)	(36,15,90)	(34,16,91)	(39,19,96)
	ec	(36,7,94)	(34,12,95)	(40,11,98)	(36,16,91)	(38,18,92)	(41,17,94)
	lf	(36,10,87)	(35,11,93)	(39,12,95)	(28,19,88)	(33,13,94)	(39,19,98)
	rf	(39,9,94)	(34,9,93)	(40,12,97)	(36,15,90)	(36,15,92)	(40,19,95)
LH	eo	(−31,3,92)	(−35,10,97)	(−38,3,98)	(−35,−4,89)	(−35,11,97)	–
	ec	(−32,3,93)	(−35,5,96)	(−39,3,97)	(−32,2,89)	(−35,12,99)	(−35,4,101)
	lf	(−35,−1,88)	(−34,12,95)	(−38,−5,93)	(−32,−2,84)	–	(−47,−20,88)
	rf	(−32,−1,88)	(−35,9,95)	(−35,12,100)	(−32,3,87)	(−30,17,96)	(−36,−2,100)
Subject 3			15 Hz			20 Hz	
RH	eo	(31,−12,76)	(30,10,92)	(34,5,88)	(27,5,83)	(37,10,94)	(33,9,86)
	ec	(29,13,90)	(30,11,96)	(32,6,86)	(27,7,84)	–	(34,10,83)
	lf	(29,10,91)	(30,10,92)	(31,8,87)	(30,6,87)	(29,8,89)	(35,9,86)
	rf	(29,10,88)	(33,10,91)	(33,9,86)	(29,5,83)	(31,11,93)	(34,8,86)
LH	eo	(−43,−13,72)	(−36,11,93)	(−40,0,86)	(−32,0,80)	(−37,12,94)	(−38,3,84)
	ec	–	(−36,11,92)	(−40,2,84)	(−33,20,84)	–	(−39,4,87)
	lf	(−27,−1,84)	(−32,11,89)	(−36,5,86)	(−29,−4,84)	(−35,13,89)	(−37,3,87)
	rf	(−30,−1,88)	(−36,12,92)	(−37,7,86)	(−31,−1,88)	(−34,11,90)	(−37,5,87)

The source locations are given in millimeters. The *x*-axis of the coordinate system passes through the preauricular points, from left to right, the *y*-axis passes through the nasion and the *z*-axis points upward from the plane determined by the *x*- and *y*-axes. Subject 4 showed almost no rhythmic activity in sensorimotor areas and is not included.
RH—right hemisphere; LH—left hemisphere.
eo—Eyes open; ec—eyes closed; lf—left finger movement; rf—right finger movement.

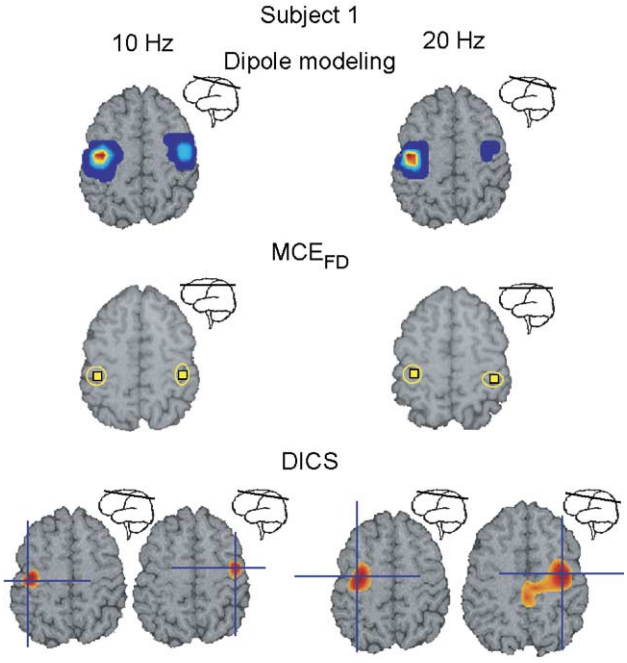

Fig. 3. Source locations of the 10-Hz (left) and 20-Hz rhythms (right) found in sensorimotor areas with the three analysis methods. The results from the dipole modeling are shown as dipole density plots superimposed on the MR images (top). The results from MCE$_{FD}$ are visualized as ellipsoids (middle). The pSPMs of the left- and right-hemisphere sources obtained with DICS are shown on separate slices (bottom). The exact location of the source is selected from the pSPM images manually, and is indicated by the cross. Subject 1, eyes-closed condition.

but was still localized in all subjects using DICS and dipole modeling.

Source removal in DICS

DICS gives the possibility to investigate weaker sources by removing the field of previously located stronger sources by including it in the noise estimate before noise normalization. It is therefore of interest to investigate how the removal of already localized sources affects identification of subsequent sources, especially in regions where several sources are located close to each other. Fig. 5 shows an example of how source removal may affect localization of subsequent sources in this kind of difficult case. In Subject 2, an extended activation was seen in the posterior regions in the eyes-closed condition, and the underlying source could be selected in two different ways. The pSPM of the first posterior source is shown superimposed on the subject's brain and the two alternatives for selecting the source are shown as blue or yellow circles. Depending on how this first source was selected (and removed), two very different solutions were obtained. The two different solutions are shown on a surface view of the subject's MR image. One of the solutions (yellow circles) corresponded very well to the solution obtained for the eyes-open condition (red circles).

Additional sources

Using DICS, additional sources were identified in the inferior sensorimotor or in the superior temporal cortex in all subjects (see Fig. 6A). The sources were found in both 10-Hz and 20-Hz frequency bands. The 20-Hz sources were often detected anterior and superior to the 10-Hz sources. The sources could be found in

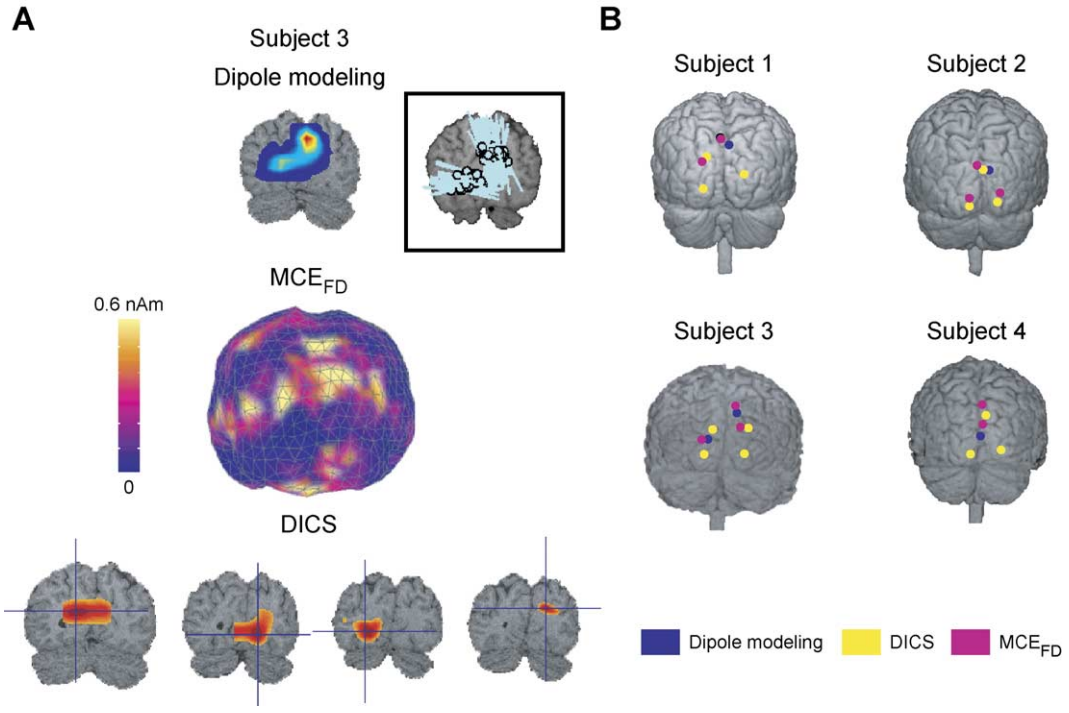

Fig. 4. (A) Sources located in the posterior region in the 10-Hz range (Subject 3, eyes-closed condition). The dipole density plot is shown on top. The black box demonstrates how the ECDs in the two clusters are oriented almost orthogonally. The results from MCE$_{FD}$ are shown projected to the surface of the BEM (see panel B, Subject 3, for the regions of interest selected from this overview). The results from DICS are displayed at the bottom. (B) All sources in the posterior regions in the 10-Hz range, determined with the three different methods (colors), are shown on a surface view of the MR images. Subjects 1 to 4, eyes closed.

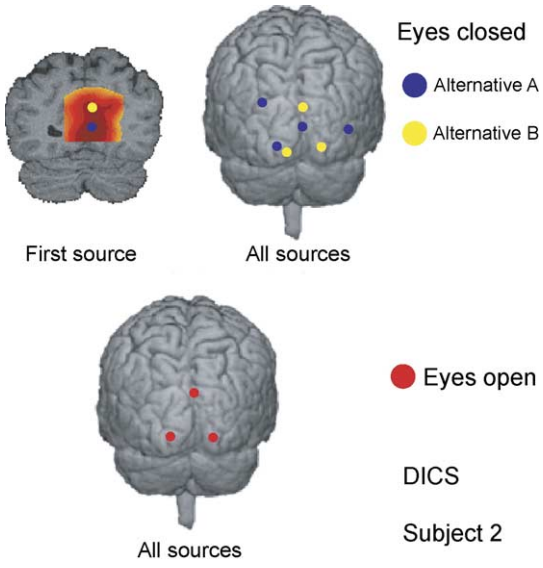

Fig. 5. Localization of posterior 10-Hz sources using DICS (Subject 2). In the eyes-closed condition (top), two different solutions were obtained (blue vs. yellow dots), depending on how the first source was chosen. The pSPM of the first posterior source is shown superimposed on the subject's brain. Alternative B (yellow dots) agreed with the solution obtained in the eyes-open condition (below, red dots).

all tasks. In many cases, however, five or more dipoles had already been removed, which reduces the reliability of these sources.

In Subject 1, the 10-Hz sources were very clear. Based on the results from DICS, the data were analyzed again using MCE_{FD} and dipole modeling. The frequency spectra of this subject showed that there was a 9-Hz spectral peak over lateral areas. Using a frequency of 9 Hz in MCE_{FD}, and a different selection of sensors in dipole modeling, these sources were now found also using the two other methods (see Fig. 6B). In Subject 3, clear temporal activity was found using all methods in the 10-Hz band. In Subjects 2 and 4, these sources were only found using DICS. The sources in the 20-Hz band were found only using DICS.

In DICS, a possible source area was also found near the frontoparietal midline in many subjects. This source in some cases interfered with source localization in the hand area. Increased power in this area was also seen in MCE_{FD}. No sources were detected in these regions using dipole modeling even when a subset of sensors was selected directly over the vertex.

Simulations

The simulations were designed to address questions that had been raised by the results from the measured data, e.g., how well the methods can discern sources that are localized close to each other and to quantify how much simultaneously active sources affect the source localization. The simulations are intended to give an overview of how the methods work in scenarios encountered in real data. Simulations showing the effect of SNR on source localization using DICS and MCE_{FD} can be found in previous papers (Gross et al., 2001; Jensen and Vanni, 2002).

Single source

For a first comparison, a single source was used. The source was placed in an area corresponding approximately to the left or to the right hand sensorimotor area, with current orientation similar to that encountered in real data. Five different source strengths were used, ranging from 2 to 15 nAm, in order to compare the sensitivity of the different methods. Table 2 shows the localization errors.

At the four highest activation strengths, the source could be localized using all methods, but at the fifth, weakest level, the source could not be found using dipole modeling (Fig. 7). As can be seen from Table 2, the source strength did not have a big impact on the localization error. The mislocalization in the *x* direction in all methods was always towards the midline.

Although the localization of the center point did not improve with increasing source strength, in DICS, a stronger source gave a

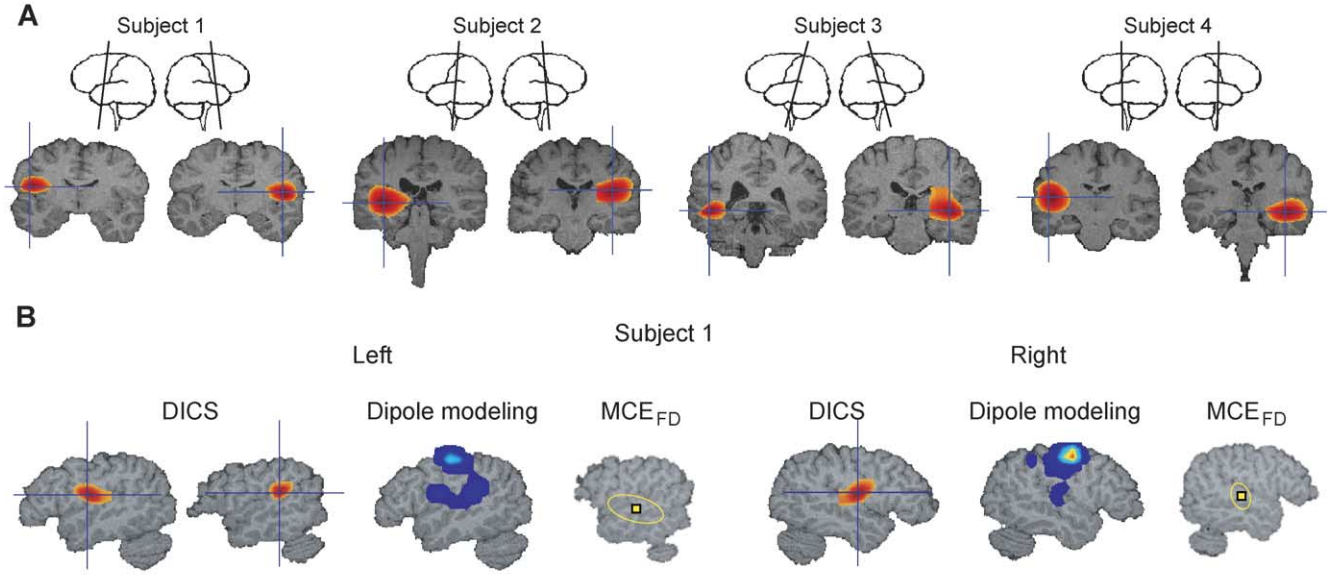

Fig. 6. (A) Examples of additional sources found in the superior temporal cortex and near the sensorimotor mouth area (10 Hz, eyes open) using DICS. (B) Additional sources found in Subject 1 (10 Hz, eyes open), comparison of the three analysis methods.

Table 2
Localization errors for simulations with a single source in the hand area

	DICS		MCE_{FD}		Dipole modeling	
[nAm]	(*x*,*y*,*z*) [mm]	Δ [mm]	(*x*,*y*,*z*) [mm]	Δ [mm]	(*x*,*y*,*z*) [mm]	Δ [mm]
Right hand (43,15,91)						
15	(43,15,92)	1	(40,21,90)	7	(41,15,90)	2 (2822)[a]
10	(40,15,88)	4	(40,15,90)	3	(41,15,90)	2 (1219)
7	(42,16,91)	2	(40,14,90)	4	(42,15,90)	2 (419)
5	(41,15,92)	2	(41,19,88)	5	(42,16,90)	2 (109)
2	(35,15,87)	9	(37,16,89)	7	–	–
Left hand (−36,9,97)						
15	(−32,10,96)	4	(−31,11,92)	7	(−35,8,97)	1 (1692)
10	(−35,7,97)	2	(−31,5,93)	8	(−35,9,97)	1 (744)
7	(−32,9,96)	4	(−33,5,97)	5	(−35,9,97)	1 (216)
5	(−34,7,97)	3	(−33,12,93)	5	(−36,9,96)	1 (34)
2	(−33,6,97)	4	(−38,11,97)	3	–	–

[a] Number of accepted dipoles.

more focal source. In dipole modeling, the localization error was smaller than in the two other methods. The main effect of increased source strength was an increase in the number of accepted dipoles. With only one active source, if the methods detected the sources at all, the location was about correct. DICS and MCE_{FD} were able to detect weaker sources than dipole modeling.

Simultaneously active sources

In measured data, sources are typically found bilaterally in the left and right sensorimotor hand areas. Simultaneously active sources in the left and right hand areas were therefore used in order to compare how much the field of one active source affects the localization of the other. In the left hemisphere, a source that could be localized well using all three methods during the single-source simulations was used. In the right hemisphere, two different source strengths were used. The localization results can be seen in Table 3. The increase in localization error was very small and the results were thus not much affected by the two sources being simultaneously active. Using dipole modeling, only slightly fewer dipoles were accepted compared to when only one dipole was active.

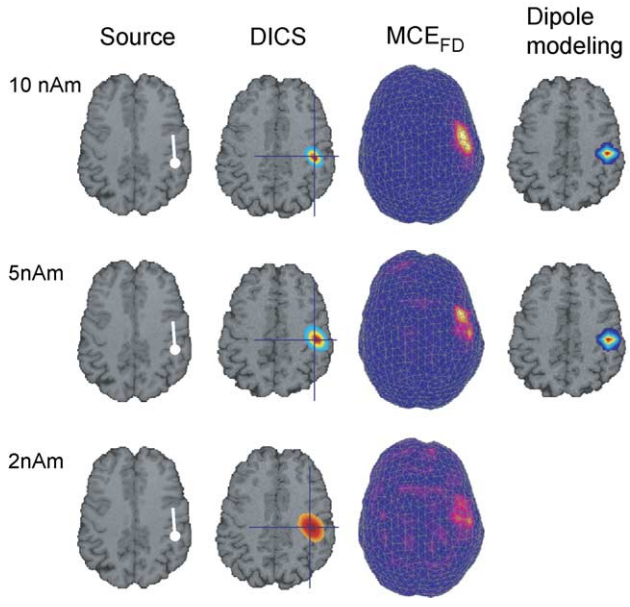

Fig. 7. Localization of a simulated source in the right hand area, with a signal strength of 10, 5, or 2 nAm, using the three analysis methods.

Separability of sources

It is sometimes difficult to assess whether a single source or two sources that are very near each other have been localized, and sometimes different methods give different results. In simulations, it is possible to test how well the methods can separate two sources. Two parallel sources were therefore placed at varying distances from each other in the parietooccipital area. Three different distances between the dipoles were used, 1, 2, and 4 cm, in order to determine at which distance the sources can be separated. A source strength of 10 nAm was used for all dipoles. The results are shown in Fig. 8.

At a distance of 1 cm between the sources, all methods detected only a single source between the two actual dipoles. In DICS, when the source in the middle was removed, two false sources were also found, one on each side of the first source. When the sources were 2 cm apart, DICS could separate the two sources, whereas MCE_{FD} and dipole modeling still gave one single source between the two real sources. When the sources were 4 cm apart, all methods could separate them. The source directions were parallel, so the sources were particularly difficult to discern.

Table 3
Location and localization error of simultaneously active sources in the left and right hand area

	Right hand (43,15,91)		Left hand (−36,9,97)	
	5 nAm		5 nAm	
	(*x*,*y*,*z*) [mm]	Δ [mm]	(*x*,*y*,*z*) [mm]	Δ [mm]
DICS	(40,15,92)	4	(−35,6,97)	3
MCE_{FD}	(37,15,88)	6	(−35,11,96)	3
Dipole modeling	(41,16,90)	2 (77)[a]	(−35,8,97)	1 (40)
	10 nAm		5 nAm	
	(*x*,*y*,*z*) [mm]	Δ [mm]	(*x*,*y*,*z*) [mm]	Δ [mm]
DICS	(40,14,87)	5	(−35,6,97)	3
MCE_{FD}	(37,15,89)	7	(−33,7,96)	3
Dipole modeling	(42,15,90)	2 (1120)	(−37,7,97)	2 (26)

[a] Number of accepted dipoles.

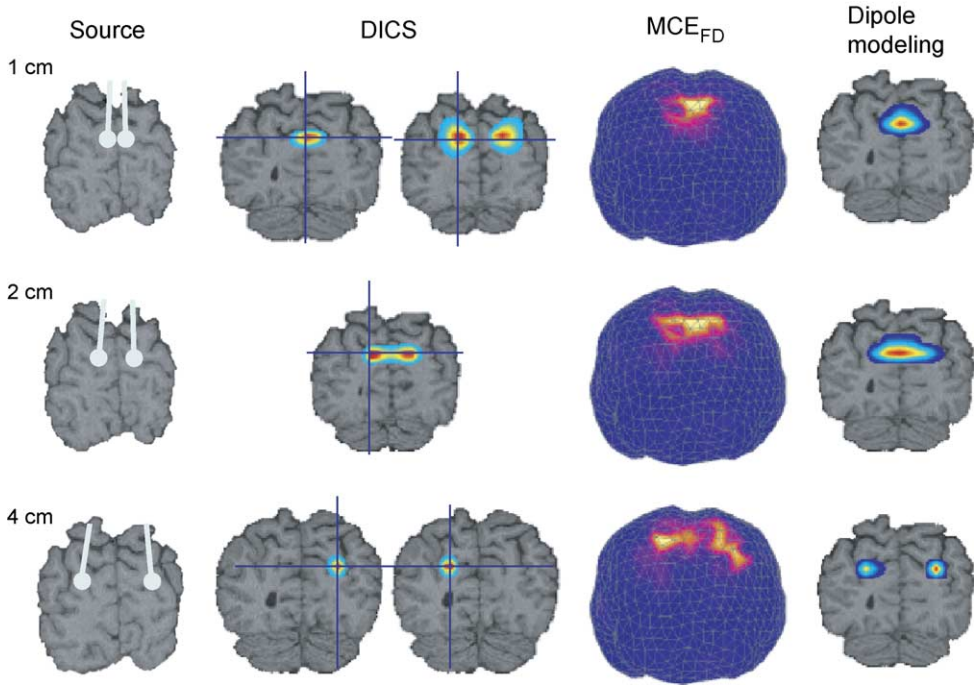

Fig. 8. Localization of two simulated sources in the parietooccipital cortex, with identical orientations of current flow, placed at a distance of 1 cm, 2 cm, and 4 cm from each other. At the 1-cm distance, none of the methods could separate the sources. With DICS, when the source in the middle was removed, two false sources were also found. At the 2-cm distance, only DICS could separate the two sources. At the 4-cm distance, all three methods could separate the two sources.

The results from the data analysis of the measured data indicated that several source areas were simultaneously active in parietal and occipital regions. Dipole modeling and MCE$_{FD}$ typically suggested one source approximately in the parietooccipital sulcus, close to the midline. In some cases, DICS found separate sources in the left and right hemisphere. Sources were found also in the left and right occipital lobes. The spatial discrimination of simultaneously active sources in MEG is, however, in the order of a few centimeters (Lütkenhöner, 1998), rendering the source localization in areas with several simultaneously active sources highly ambiguous. Four sources were therefore used to compare the responses of the different methods. Table 4 shows the result of a simulation where two sources were placed near the parietooccipital sulcus, one in each hemisphere, and two sources near the calcarine sulcus, again one in each hemisphere. The source strength of the dipoles near the parietooccipital sulcus was 10 nAm, whereas the source strength of the dipoles in the occipital lobes was 5 nAm. The orientation of current flow in the occipital source areas was perpendicular to the current flow in parietooccipital source areas.

With DICS, all four sources could be separated. Removal of sources a few centimeters away did not seem to have a large impact on the localization of subsequent sources. Using MCE$_{FD}$, two distinct source areas could be separated, one in the parietooccipital sulcus and one in the occipital lobes. In dipole modeling, a single-source cluster was found between the two parietooccipital sources. The occipital sources could not be detected at all.

Several simultaneously active sources

Using DICS, additional sources were found in the measured data that could not be detected using the other two methods. In most cases, sources were found in the inferior sensorimotor or superior temporal cortex. Also, more sources could be separated in the parietooccipital areas than using the other methods. Whether these sources are true sources or merely noise can be difficult to tell. In the last set of simulations, sources were therefore placed in areas where they had been detected using DICS. Sources were placed bilaterally in the sensorimotor hand area, the parietooccipital sulcus, the occipital lobe, and near the sensorimotor mouth area. The activation strength of the sources near the hand and parietooccipital areas was 10 nAm, whereas the strength of the sources near the mouth and in the occipital areas was 5 nAm. The same simulation was run ten times with different noise and time

Table 4
Simulation using two dipoles near the parietooccipital sulcus with source strength 10 nAm, and two dipoles near the calcarine sulcus with source strength 5 nAm

Source	DICS		MCE$_{FD}$		Dipole modeling	
(x,y,z) [mm]	(x,y,z) [mm]	Δ [mm]	(x,y,z) [mm]	Δ [mm]	(x,y,z) [mm]	Δ [mm]
(14,−43,85)	(15,−47,83)	5	(−1,−41,81)	16	(−1,−44,83)	15
(−12,−45,87)	(−9,−47,84)	5		13		12
(−10,−62,55)	(−5,−62,55)	5	(0,−49,60)	18		
(16,−54,53)	(20,−61,55)	8		18		

series for the simulated sources, and the mean location of the sources was calculated. Fig. 9 shows the results of one of the runs. The results across runs can be seen in Table 5.

Using DICS, the hand and the parietooccipital sources could be localized with localization errors of only a few millimeters.

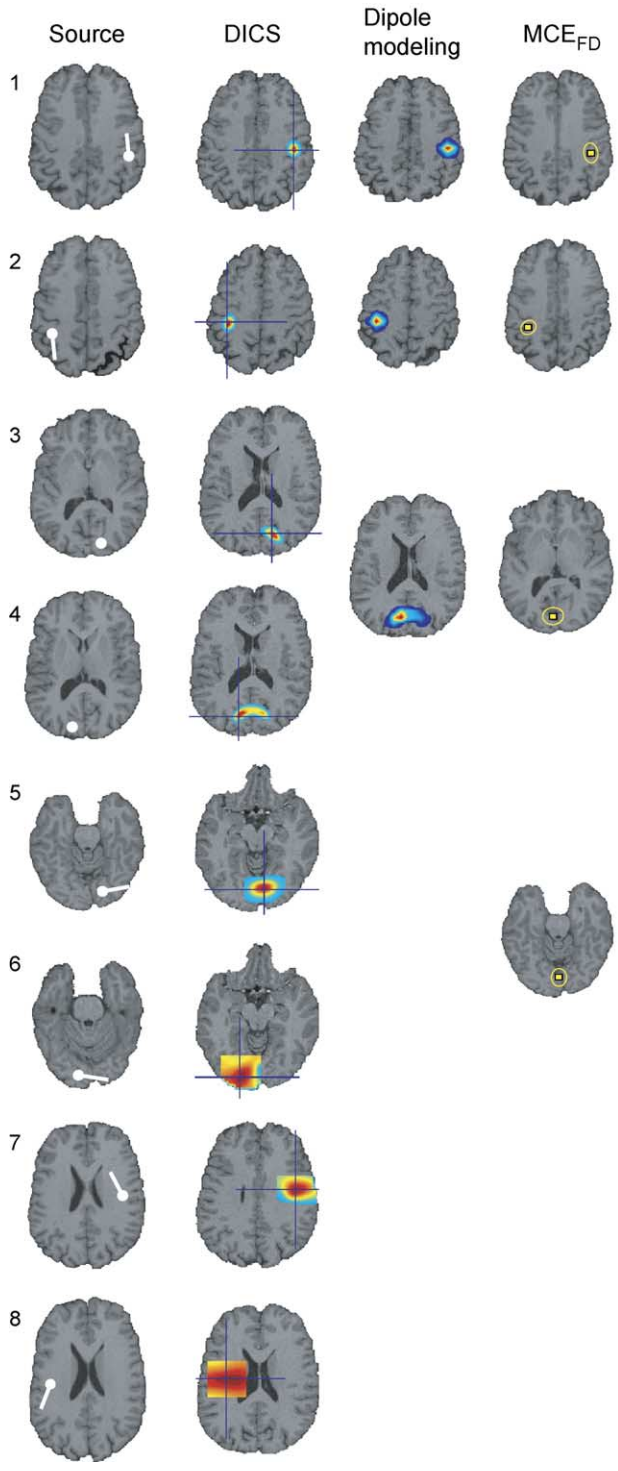

Fig. 9. Localization of a set of simulated sources in both hemispheres in the sensorimotor hand area (sources 1 and 2), near the parietooccipital sulcus (3 and 4), in the occipital lobe (5 and 6), and near the sensorimotor mouth area (7 and 8), using the three methods.

The weaker sources near the mouth areas and in the occipital areas were found in nine runs out of ten, and the localization errors were larger (see Table 5). Using MCE$_{FD}$, four sources were found. The localization errors for the sources in the hand area were below 1 cm. Two source areas were identified in the posterior regions, one near the midline, close to the parietooccipital sulcus, between the two actual sources, and another, weaker area was found in the occipital regions, again between the two original sources. The sources near the mouth area were not detected at all.

Using dipole modeling, only three source areas were found. The sources in the hand areas were both localized very accurately, with an error below 2 mm. In the posterior regions, only one single-source area could be found, near the parietooccipital sulcus, between the two simulated sources. The sources in the mouth and the occipital areas could not be detected. It seems that DICS, indeed, could localize sources that the other methods did not detect.

Discussion

In the real MEG data, sources were localized bilaterally in the sensorimotor hand areas with all three techniques. In the posterior regions, sources were found near the parietooccipital sulcus and in the occipital lobes. Although interindividual differences emerged in the locations of sources, the main results were consistent between the methods. In the hand area, the differences between the methods were typically a few millimeters, but in the parietooccipital area, they were up to several centimeters. DICS typically found separate sources near the parietooccipital sulcus and in the occipital lobes, whereas the activation pattern was more difficult to interpret using MCE$_{FD}$ and dipole modeling. Using dipole modeling, the source clusters could in some cases be separated according to the orientation of current flow. The somewhat ambiguous results from the posterior regions suggest a more complex activation pattern in the parietooccipital areas than a single source can account for, making the selection of the correct source areas increasingly difficult. Earlier studies have shown that there are multiple generators of alpha activity in the posterior parts of the cerebrum, with activity arising near the parietooccipital areas and in the calcarine sulcus (Hari and Salmelin, 1997; Salenius et al., 1995).

Using DICS, possible sources were found also in the superior temporal and in the inferior sensorimotor cortex in the 10- and 20-Hz frequency bands. The 10-Hz sources found in the temporal areas seem to correspond both in frequency and location to the tau rhythm. The tau rhythm is generally not seen in the eyes-open/eyes-closed condition, but may show reactivity to auditory responses (Lehtelä et al., 1997). This could explain the activity during the finger movement tasks, since the finger movements were paced by a tone to the left ear. Sources in the 20-Hz band are not generally seen in spontaneous data in these areas. However, following mouth movements, a transient increase in rhythmic activity is seen in the mouth area (Salmelin et al., 1995). It would thus be physiologically plausible that the 20-Hz sources would arise from these areas. However, the possibility that these sources result from insufficient source removal cannot be entirely excluded.

In simulations, the source removal in DICS was found to be very accurate, enabling the separation of two sources that were

Table 5
Mean localization error

	Source	DICS		MCE_{FD}		Dipole modeling	
	(*x*,*y*,*z*) [mm]	(*x*,*y*,*z*) [mm]	Δ [mm]	(*x*,*y*,*z*) [mm]	Δ [mm]	(*x*,*y*,*z*) [mm]	Δ [mm]
RH	(43,15,91)	(43,16,90)	2	(36,16,87)	8	(41,15,90)	2
LH	(−36,9,97)	(−36,11,98)	2	(−33,12,92)	7	(−36,9,96)	1
RP	(14,−43,85)	(13,−41,89)	4	(−2,−39,81)	17	(0,−42,82)	14
LP	(−12,−45,87)	(−11,−45,90)	3		13		14
RO	(16,−54,53)	(25,−56,50)	10	(−1,−51,58)	18		
LO	(−10,−62,55)	(−10,−61,52)	4		15		
RM	(40,30,70)	(47,41,69)	13				
LM	(−40,25,70)	(−42,35,66)	11				

Simulations with dipoles near the right hand area (RH, 10 nAm), the left hand area (LH, 10 nAm), the right parietooccipital sulcus (RP, 10 nAm), the left parietooccipital sulcus (LP, 10 nAm), in the right occipital lobe (RO, 5 nAm), in the left occipital lobe (LO, 5 nAm), near the right mouth area (RM, 5 nAm), and the left mouth area (LM, 5 nAm).

located only 2 cm apart. In real data, however, source removal proved difficult in some cases. When removing a source, only the principal component of the current flow was taken into account. The benefit of this approach is that it is possible to identify sources that are located very close to each other. However, the potential risk is that the already localized source is not completely removed and the remaining field may thus cause errors in the localization of subsequent sources. Another approach would be to remove all activity at that location, but in that case, sources situated very close to each other may go undetected.

The results from the simulations indicate that simultaneously active sources in the left and right hand areas affect source localization very little, whereas sources close to each other, e.g., in the mouth and the hand areas, or in the posterior parietal and the occipital areas, affect source localization in dipole modeling and MCE_{FD} so that only the stronger source is detected. In DICS, also the weaker sources can be detected, but the localization error increases with the number of sources removed.

In neither MCE_{FD} nor DICS need assumptions be made about how many sources are active or in which general areas these sources can be found. In dipole modeling, the general regions of interest must be defined a priori from the frequency spectra. In difficult situations, MCE_{FD} could be used to determine which subsets of sensors to use when analyzing the data using dipole modeling. Both MCE_{FD} and DICS suffer from the significance problem, i.e., there are no good criteria for which sources one should accept and which reject in an individual subject and when only one experimental condition is evaluated. Recently, a method has been proposed for testing whether source areas of rhythmic activity differ between two experimental conditions. Gross et al. (2003), using a bootstrapping method, calculated the confidence volume for a location in the brain, which is a measure of the uncertainty of localization. Another new method allows for making statistical inference at the group level in experimental designs with multiple conditions (Singh et al., 2003). Here, a measure of differential activation can be obtained for each voxel using a spatial filter (SAM), and its significance at a group level is estimated using nonparametric permutation testing. These methods could be explored further.

Summary

It appears that with a fairly simple, single area of activation, the methods perform equally well, but with a more complicated distribution of active areas, the differences between the methods become evident. Using MCE_{FD}, sources could be found simultaneously in parietooccipital areas and bilaterally in hand areas. MCE_{FD} was thus the fastest of the three methods. However, it was difficult to separate sources in posterior regions. Since the scaling is done according to the stronger source, a weaker source might not be detected. DICS gives the possibility to investigate sources located close to each other by removing the field of previously located stronger sources. Indeed, in simulations, DICS proved to be able to separate the sources better than the other methods. With DICS, weaker sources could also be detected. Using dipole modeling, the dipole clusters from sources located close to each other often overlapped. However, they could sometimes be separated according to the orientation of current flow. In simulations with sources in the hand area, the smallest localization errors were obtained with dipole modeling.

Acknowledgments

This work was supported by the Jenny and Antti Wihuri Foundation, the Ministry of Education of Finland, the Academy of Finland (Finnish Centre of Excellence Program 2000–2005), the James S. McDonnell Foundation, and the Sigrid Jusélius Foundation.

References

Adrian, E.D., Matthews, B.H.C., 1934. The Berger rhythm: potential changes from the occipital lobes in man. Brain 57, 355–385.

Berger, H., 1929. Über das Elektroenkephalogram des Menschen. Arch. Psychiatr. Nervenkrankh. 87, 527–570.

Chatrian, G.E., Petersen, M.C., Lazarte, J.A., 1959. The blocking of the rolandic wicket rhythm and some central changes related to movement. Electroencephalogr. Clin. Neurophysiol. 11, 497–510.

Cheyne, D., Gaetz, W., Garnero, L., Lachaux, J.-P., Ducorps, A., Schwartz, D., Varela, F., 2003. Neuromagnetic imaging of cortical oscillations accompanying tactile stimulation. Brain Res. Cogn. Brain Res. 17, 599–611.

Gastaut, H., 1952. Etude electrocorticographique de la reactivite des rhythmes rolandiques. Rev. Neurol. 87, 176–182.

Gross, J., Kujala, J., Hämäläinen, M., Timmermann, L., Schnitzler, A., Salmelin, R., 2001. Dynamic imaging of coherent sources: studying neural interactions in the human brain. Proc. Natl. Acad. Sci. U. S. A. 98, 694–699.

Gross, J., Timmermann, L., Kujala, J., Salmelin, R., Schnitzler, A., 2003. Properties of MEG tomographic maps obtained with spatial filtering. NeuroImage 19, 1329–1336.

Hari, R., Salmelin, R., 1997. Human cortical oscillations: a neuromagnetic view through the skull. Trends Neurosci. 20, 44–49.

Hämäläinen, M.S., Sarvas, J., 1989. Realistic conductivity geometry model of the human head for interpretation of neuromagnetic data. IEEE Trans. Biomed. Eng. 36, 165–171.

Hämäläinen, M., Hari, R., Ilmoniemi, R.J., Knuutila, J., Lounasmaa, O.V., 1993. Magnetoencephalography—theory, instrumentation, and applications to non-invasive studies of the working human brain. Rev. Mod. Phys. 65, 413–497.

Jensen, O., Vanni, S., 2002. A new method to identify multiple sources of oscillatory activity from magnetoencephalographic data. NeuroImage 15, 568–574.

Kaukoranta, E., Hämäläinen, M., Sarvas, J., Hari, R., 1986. Mixed and sensory nerve stimulations activate different cytoarchitectonic areas in the human primary somatosensory cortex SI. Neuromagnetic recordings and statistical considerations. Exp. Brain Res. 63, 60–66.

Lehtelä, L., Salmelin, R., Hari, R., 1997. Evidence for reactive magnetic 10-Hz rhythm in the human auditory cortex. Neurosci. Lett. 222, 111–114.

Lounasmaa, O.V., Hämäläinen, M., Hari, R., Salmelin, R., 1996. Information processing in the human brain: magnetoencephalographic approach. Proc. Natl. Acad. Sci. U. S. A. 93, 8809–8815.

Lütkenhöner, B., 1998. Dipole separability in a neuromagnetic source analysis. IEEE Trans. Biomed. Eng. 45, 572–581.

Mäkelä, J.P., Salmelin, R., Kotila, M., Salonen, O., Laaksonen, R., Hokkanen, L., Hari, R., 1998. Modification of neuromagnetic cortical signals by thalamic infarctions. Electroencephalogr. Clin. Neurophysiol. 106, 433–443.

Matsuura, K., Okabe, Y., 1995. Selective minimum-norm solution of the biomagnetic inverse problem. IEEE Trans. Biomed. Eng. 42, 608–615.

Niedermeyer, E., 1990. Alpha-like rhythmical activity of the temporal lobe. Clin. Electroencephalogr. 21, 210–224.

Niedermeyer, E., 1993. The normal EEG of the waking adult. In: Niedermeyer, E., Lopes da Silva, F. (Eds.), Electroencephalography. Basic principles, clinical applications and related fields. Williams and Wilkins, Baltimore, MD.

Perez-Borja, C., Chatrian, G.E., Tyce, F.A., Rivers, M.H., 1962. Electrographic patterns of the occipital lobe in man: a topographic study based on use of implanted electrodes. Electroencephalogr. Clin. Neurophysiol. 14, 171–182.

Robinson, S.E., Vrba, J., 1999. Functional neuroimaging by Synthetic Aperture Magnetometry (SAM). In: Yoshimoto, T., Kotani, M., Kuriki, S., Karibe, H., Nakasato, N. (Eds.), Recent Advances in Biomagnetism. Tohoku Univ. Press, Sendai.

Salenius, S., Kajola, M., Thompson, W.L., Kosslyn, S., Hari, R., 1995. Reactivity of magnetic parieto-occipital alpha rhythm during visual imagery. Electroencephalogr. Clin. Neurophysiol. 95, 453–462.

Salenius, S., Portin, K., Kajola, M., Salmelin, R., Hari, R., 1997. Cortical control of human motoneuron firing during isometric contraction. J. Neurophysiol. 77, 3401–3405.

Salmelin, R., Hämäläinen, M., 1995. Dipole modelling of MEG rhythms in time and frequency domains. Brain Topogr. 7, 251–257.

Salmelin, R., Hari, R., 1994a. Characterization of spontaneous MEG rhythms in healthy adults. Electroencephalogr. Clin. Neurophysiol. 91, 237–248.

Salmelin, R., Hari, R., 1994b. Spatiotemporal characteristics of sensorimotor neuromagnetic rhythms related to thumb movement. Neuroscience 60, 537–550.

Salmelin, R., Sams, M., 2002. Motor cortex involvement during verbal versus non-verbal lip and tongue movements. Hum. Brain Mapp. 16, 81–91.

Salmelin, R., Hämäläinen, M., Kajola, M., Hari, R., 1995. Functional segregation of movement-related rhythmic activity in the human brain. NeuroImage 2, 237–243.

Salmelin, R., Schnitzler, A., Schmitz, F., Freund, H.J., 2000. Single word reading in developmental stutterers and fluent speakers. Brain 123, 1184–1202.

Singh, K.D., Barnes, G.R., Hillebrand, A., Forde, E.M., Williams, A.L., 2002. Task-related changes in cortical synchronization are spatially coincident with the hemodynamic response. NeuroImage 16, 103–114.

Singh, K.D., Barnes, G.R., Hillebrand, A., 2003. Group imaging of task-related changes in cortical synchronization using nonparametric permutation testing. NeuroImage 19, 1589–1601.

Taniguchi, M., Kato, A., Fujita, N., Hirata, M., Tanaka, H., Kihara, T., Ninomiya, H., Hirabuki, N., Nakamura, H., Robinson, S.E., Cheyne, D., Yoshimine, T., 2000. Movement-related desynchronization of the cerebral cortex studied with spatially filtered magnetoencephalography. NeuroImage 12, 298–306.

Tiihonen, J., Kajola, M., Hari, R., 1989. Magnetic mu rhythm in man. Neuroscience 32, 793–800.

Tiihonen, J., Hari, R., Kajola, M., Karhu, J., Ahlfors, S., Tissari, S., 1991. Magnetoencephalographic 10-Hz rhythm from the human auditory cortex. Neurosci. Lett. 129, 303–305.

Uutela, K., Hämäläinen, M., Somersalo, E., 1999. Visualization of magnetoencephalographic data using minimum current estimates. NeuroImage 10, 173–180.

Van Veen, B.D., van Drongelen, W., Yuchtman, M., Suzuki, A., 1997. Localization of brain electrical activity via linearly constrained minimum variance spatial filtering. IEEE Trans. Biomed. Eng. 44, 867–880.